Advanced core/multishell germanium/silicon nanowire heterostructures: The Au-diffusion bottleneck

Shadi A. Dayeh,[1,a)] Nathan H. Mack,[2] Jian Yu Huang,[3] and S. T. Picraux[1]

[1]*Center for Integrated Nanotechnologies, Los Alamos National Laboratory, MS K771 Los Alamos, New Mexico 87544, USA*
[2]*Physical Chemistry and Applied Spectroscopy, Los Alamos National Laboratory, MS J569 Los Alamos, New Mexico 87544, USA*
[3]*Center for Integrated Nanotechnologies, Sandia National Laboratories, MS 1303 Albuquerque, New Mexico 87185, USA*

Synthesis of germanium/silicon (Ge/Si) core/shell nanowire heterostructures is typically accompanied by unwanted gold (Au) diffusion on the Ge nanowire sidewalls, resulting in rough surface morphology, undesired whisker growth, and detrimental performance of electronic devices. Here, we advance understanding of this Au diffusion on nanowires, its diameter dependence and its kinetic origin. We devise a growth procedure to form a blocking layer between the Au seed and Ge nanowire sidewalls leading to elimination the Au diffusion for *in situ* synthesis of high quality Ge/Si core/shell heterostructures. © *2011 American Institute of Physics*. [doi:10.1063/1.3567932]

Radial heterostructured nanowires (NWs) offer the possibility of engineering surface effects, strain, energy band edge, and modulation-doping of one-dimensional (1D) structures with unprecedented control for electronic and optoelectronic devices. Realization of such core/shell heterostructures and resulting performances, particularly, for the silicon-germanium material system, is challenging due to the diffusion of the Au growth-mediating seed during Si shell deposition. While both Si and Ge NWs can be grown by the vapor-liquid-solid (VLS) method using liquid Au alloy droplets as the catalytic growth medium, the required temperatures for wire or shell growth are quite different ($\sim 300\,^\circ$C for Ge and $500\,^\circ$C for Si).[1] This disparity in synthesis temperatures has resulted in highly detrimental Au diffusion when growing shells at higher temperature, such as for the Ge core/Si shell heterostructures.[2] To inhibit Au diffusion on NW sidewalls, previous approaches have either introduced O_2 during growth[3] or etching of the Au seed *ex situ* prior to growing Si shells,[4] both of which introduce contaminants that adversely affect the NW properties. Here, we advance understanding of this Au diffusion on nanoscale structures and solve the problem by the low temperature formation of a Si segment between the liquid Au catalyst and Ge NW before the shell growth. This approach is shown to energetically block the otherwise rapid Au diffusion along the Ge surface at the required shell growth temperatures. We demonstrate through chemical and structural analysis the detrimental consequences of this diffusion without a blocking layer, its nanoscale diameter dependence, and the effectiveness of our solution for *in situ* growth of Ge/Si heterostructured NWs.

Optimized growth of the Ge NW cores was performed in a two-step temperature process[5] in which the Ge NW growth is initiated near the Au–Ge eutectic point ($\sim 360\,^\circ$C) and the temperature was quickly ramped down to $\sim 280\,^\circ$C to reduce material deposition on the NW sidewalls and maintain 1D growth mediated by the liquid Au–Ge catalytic

nanoparticles. Figures 1(a)–1(d) show postgrowth transmission electron microscope (TEM) images near the tips of different diameter Ge NWs grown using this procedure. For core/shell NW growth, it is generally desired to stop the axial elongation of the NW core and initiate vapor-solid (thin-film) growth on the NW sidewalls.[6] For this process, the growth temperature has to be raised sufficiently for decomposition of the precursor molecules used for shell deposition, and in the case of Si, the shell deposition temperature is typically well above the Au–Ge eutectic temperature. As the temperature is ramped up, it is energetically favorable for
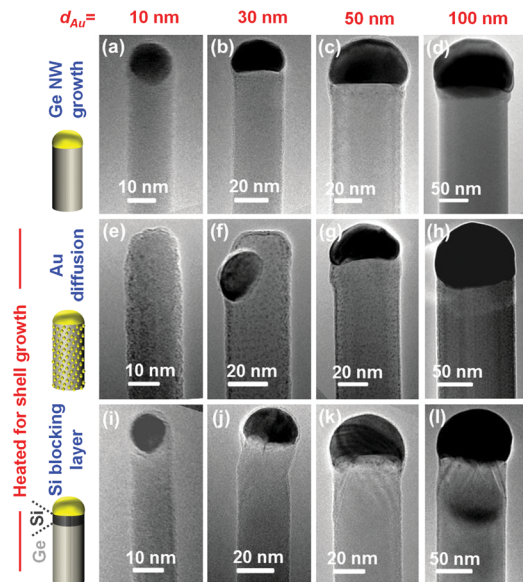
FIG. 1. (Color online) [(a)–(d)] TEM images of Ge NWs grown at $276\,^\circ$C from 10 nm, 30 nm, 50 nm, and 100 nm Au nanoparticles, respectively. No Au diffusion is observed under such growth conditions. [(e)–(h)] TEM images of Ge NWs grown at $276\,^\circ$C and subject to a temperature ramp-up to $410\,^\circ$C; Au diffusion is evident throughout all diameters with total loss of Au nanoparticle for the smallest diameter in (e), and relocation of Au nanoparticle for the 30 nm diameter NW in (f). (i)–(l) same as in (e)–(h), however, with a Si interface layer deposited at only $276\,^\circ$C which blocks Au diffusion. Note that the volumes of the Au nanoparticles in (i)–(l) are similar to those in (a)–(d), unlike (e)–(h), where Au diffusion reduces the total Au nanoparticle volume.

a)Electronic mail: shadi@lanl.gov.

atomic diffusion of Au from the Au–Ge liquid growth seed to occur along the NW sidewalls [Figs. 1(e)–1(h)]. Note that from Figs. 1(a)–1(h), we show that Au diffusion on the Ge NW sidewalls occurs after growth of the Ge NW core during the ramp up to a temperature that is suitable for Si or Ge shell growth, and is to be distinguished from previously reported high temperature or low pressure NW growth conditions where Au diffusion[7,8] can occur concurrently with NW VLS growth and the NW morphology is adversely compromised. In addition, atomic hydrogen passivation which has been noted to cause dewetting of Au on Si surfaces[9] does not inhibit Au diffusion on the Ge NW surfaces, as deduced from our temperature ramp experiments to the Si growth temperature in H_2 or GeH_4 ambient where in both cases we observed Au diffusion to still occur.

Since Si surface facets have a higher surface energy than Ge,[10] Au diffusion on the Si surface is expected to be less facile than on the Ge surface. Thus, the introduction of a thin Si layer beneath the Au growth seed is anticipated to create an energy barrier to the Au diffusion down the Ge NW sidewalls. We employ the catalytic effect of the Au nanoparticle to locally decompose SiH_4 at the Ge NW growth temperature (276 °C). When the temperature was ramped to 410 °C, no Au diffusion occurred as depicted in Figs. 1(i)–1(l), in dramatic contrast to the situation where no Si interfacial barrier layer was grown [Figs. 1(e)–1(h)].

To further elucidate and verify the role of the Si interfacial layer in blocking Au diffusion on the Ge NW surface, high angle annular dark field (HAADF) scanning TEM (STEM) analysis of the 30 nm diameter Ge NWs was performed as shown in Fig. 2. For the as-grown NW [Fig. 2(a)], no Au was observed on the NW sidewalls and energy dispersive x-ray (EDX) spectra $\sim$100 nm below the Au seed [marked as point 1 in Fig. 2(a)] showed only the Ge-L peak [spectrum 1 of Fig. 2(d)]. For the Ge NW that was subject to the 410 °C temperature ramp [Fig. 2(b)], textured bright dots corresponding to Au nanoparticles on the NW sidewalls are visible and the corresponding EDX spectra showed both Ge-L and Au-M peaks [Fig. 2(d), spectrum 2]. For the case where a SiH_4 flow was introduced at 276 °C prior to a temperature ramp in vacuum to 410 °C [Fig. 2(c)], no bright dots were observed on the NW sidewalls, in contrast to the situation in Fig. 2(b), and the EDX spectra from the NW sidewalls showed only a Ge-L peak [spectrum 3 of Fig. 2(d)]. EDX spectra taken directly underneath the Au seed for Fig. 2(c) showed Si-K and Au-M peaks, as expected, supporting the inference that a Si-rich interfacial layer inhibits Au diffusion. Detailed EDX analyses on several other NWs have shown that the Au growth seed is Si-rich and that a Si-rich GeSi interfacial layer underneath the Au quickly diminishes to pure Ge, a few tens of nanometer below the Au growth seed.

The complete loss of Au in the case of the smallest Ge NW diameter in Fig. 1(e) indicates that the Au diffusion on the Ge NW sidewalls depends on the lowest energy in the end-state configuration, which in turn is dependent on the NW diameter. To support this argument and further understand the role of the Si blocking layer in eliminating Au diffusion on Ge NW sidewalls, we use the den Hertog *et al.*[11] treatment to determine the relative lowest surface energy for a Au–Ge monolayer at the NW tip or the NW sidewalls. The
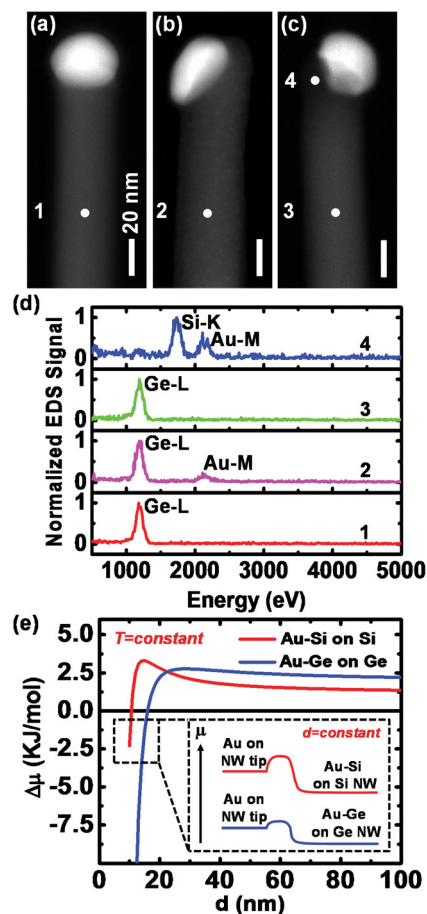
FIG. 2. (Color online) [(a)–(d)] HAADF STEM images of (a) as-grown 30 nm diameter Ge NWs at a temperature of 276 °C showing the Au nanoparticle only at the tip, (b) similar NWs heated to 410 °C after growth resulting in Au seed relocation and Au diffusion on the NW sidewalls (textured surface of bright dots), and (c) similar NWs after first depositing a Si interfacial layer at 276 °C after NW growth, then followed by temperature ramp-up to 410 °C in vacuum; no Au diffusion is observed. (d) Normalized EDX spectra at points 1–4 marked in (a)–(c) showing no Au detection in spectra 3 of the Ge NW with the Si interfacial layer of (c). (e) Comparison of Au diffusion preference on Ge and on Si NW sidewalls according to Eq. (1). The predicted onset for Au diffusion (negative $\Delta\mu$) for Au–Ge on Ge occurs at a larger diameter than that for the onset of Au diffusion on Si. Inset is a schematic illustrating a smaller energy barrier for Au to diffuse on Ge NW surface than on Si.

chemical potential difference $\Delta\mu$ of a monolayer of Au-y eutectic, where y can be either Ge or Si, from the NW surface to its tip can be expressed as

$$\Delta\mu = \mu_{\text{Au-}y}^{\text{Surf}} - \mu_{\text{Au-}y}^{\text{Tip}} = \frac{2\Omega_{\text{Au}}}{d}\left(\sigma_{\text{Au-}y^{(l)}\text{ on }y^{(s)}}^{s} - 2\sigma_{\text{Au-}y(\text{eutectic})}^{l}\right) + 4|\Delta H|x_y^2 x_{\text{Au}}, \quad (2)$$

where Ω_{Au} is the atomic volume of Au, d is the NW diameter, $\sigma_{\text{Au-}y^{(l)}\text{ on }y^{(s)}}^{s}$ is the surface energy density of a monolayer of liquid Au-y alloy on the solid y NW surface, and $2\sigma_{\text{Au-}y(\text{eutectic})}^{l}$ is the surface energy density of a monolayer of Au-y in the molten growth seed, ΔH is the enthalpy of mixing of Au and y, and x_y is the compositional fraction of y in Au. In Eq. (1) a negative $\Delta\mu$ implies Au diffusion is energetically favored and arises as the first term, which is negative, and increases at smaller diameters. The Au–Ge and Au–Si temperature-dependent surface energy densities[12] and enthalpies of mixing,[13,14] as well as the diameter-dependent Au seed composition[15] are taken into account in the present
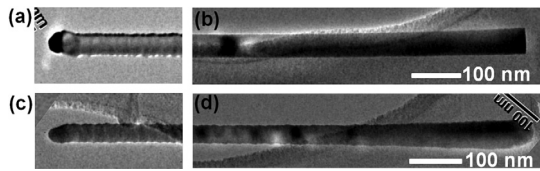
FIG. 3. Temperature ramp to 410 °C followed by Ge shell growth for 50 s without anneal [(a) NW tip and (b) base], and with 10 min anneal at 410 °C [(c) and (d)]. Rough morphology indicates extent of Au diffusion (a, c, d). Note total loss of Au in (c).

case. The addition of the diameter-dependent Au seed composition to the den Hertog model shifts the negative $\Delta\mu$ region for Si to smaller diameters, increasing the stability for Au on Si compared to Ge as shown in Fig. 2(e), consistent with our observed results. We also note that the first term in Eq. (1) increases rapidly at very small diameters, leading to a negative $\Delta\mu$ and enhanced Au diffusion, consistent with the observed greater loss of Au from the NW tip at smaller diameters as shown for Ge in Figs. 1(e)–1(h). It is worth noting that at small diameters, the commonly observed growth orientation is [110] and [211],[16] which typically results partly in lower energy {111} facets[17] than the {110} facets of [111] oriented NWs. This will also lead to an increased negative $\Delta\mu$ value and rapid Au diffusion for smaller diameter NWs.

Without the use of a Si interfacial barrier layer, total loss of Au from larger diameter Ge NW tips occur for longer annealing times. For example, a temperature ramp to 410 °C in 5 min followed by 50 sec Ge shell was observed to result in Au diffusion a distance of ∼700 nm down the sidewalls of a 30 nm diameter Ge NW from the Au tip [Figs. 3(a)–3(c)], whereas holding the temperature constant at 410 °C for an additional time of 10 min with everything else kept the same resulted in Au diffusion throughout the entire NW length of ∼2.3 μm [Figs. 3(d)–3(f)]. To further characterize this effect, annealing was carried out to different peak temperatures after deposition of the Si layer. Our results show that the Si interfacial layer can serve as an energy barrier for Au diffusion up to a temperature of ∼490 °C at which point Au dots begin to appear on the NW surface (Fig. 4). With this comprehensive understanding of Au diffusion on NW surfaces, high quality Ge/Si core/multishell Ge/Si heterostructure NWs can be grown and correlated with transport behavior.

We presented results for overcoming the degradation due to Au diffusion during the growth of Ge/Si core/multishell heterostructured NWs. Both diameter and temperature dependences of Au diffusion on Ge NW sidewalls during temperature ramp-up for shell depositions are shown to be consistent with theoretical modeling and the effect is shown to be of kinetic origin. To block such Au diffusion, we used interface engineering to deposit a low-temperature Si layer,
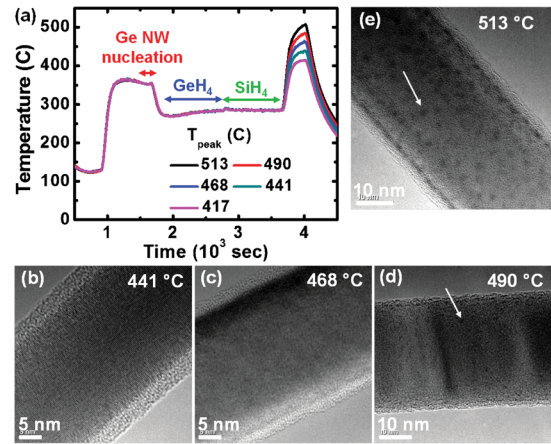
FIG. 4. (Color online) Characterization of the stability of the Au seed on top of a 30 nm diameter Ge NW as a function of temperature. (a) Temperature profile of Ge NW nucleation and growth steps, followed by a low temperature deposition of a Si barrier layer step, and ramp up to different peak temperatures. [(b), (c), (d), and (e)] TEM images near the Ge NW tip for these growths whose temperature profiles are shown in (a). Clear dark contrast (marked by arrow) on the NW surface was observed near 490 °C illustrating that the Si interfacial barrier layer withstands Au diffusion up to ∼490 °C. The low contrast shell on the Ge NW surface is due to carbon deposition at high intensity electron beam irradiation.

as energy barrier for Au diffusion. The detailed studies presented here provide a unique route for the synthesis of optimized morphology of energy band edge engineered devices.

[1]S. T. Picraux, S. A. Dayeh, P. Manandhar, D. E. Perea, and S. G. Choi, J. Metals **62**, 35 (2010).
[2]I. A. Goldthorpe, A. F. Marshall, and P. C. McIntyre, Nano Lett. **8**, 4081 (2008).
[3]S. Kodambaka, J. B. Hannon, R. M. Tromp, and F. M. Ross, Nano Lett. **6**, 1292 (2006).
[4]I. A. Goldthorpe, A. F. Marshall, and P. C. McIntyre, Nano Lett. **9**, 3715 (2009).
[5]D. Wang, Q. Wang, A. Javey, R. Tu, H. Dai, H. Kim, P. C. McIntyre, T. Krishnamohan, and K. C. Saraswat, Appl. Phys. Lett. **83**, 2432 (2003).
[6]S. A. Dayeh, E. T. Yu, and D. Wang, Nano Lett. **9**, 1967 (2009).
[7]J. B. Hannon, S. Kodambaka, F. M. Ross, and R. M. Tromp, Nature (London) **440**, 69 (2006).
[8]P. Madras, E. Dailey, and J. Drucker, Nano Lett. **10**, 1759 (2010).
[9]E. Dailey and J. Drucker, J. Appl. Phys. **105**, 064317 (2009).
[10]Q. Jiang, H. M. Lu, and M. Zhao, J. Phys.: Condens. Matter **16**, 521 (2004).
[11]M. I. den Hertog, J.-L. Rouviere, F. Dhalluin, P. J. Desre, P. Gentile, P. Ferret, F. Oehler, and T. Baron, Nano Lett. **8**, 1544 (2008).
[12]Y. V. Naidich, V. M. Perevertailo, and L. P. Obushchak, Powder Metallurgy and Metal Ceramics **14**, 567 (1975).
[13]H. Okamoto and T. B. Massalski, J. Phase Equilib. **5**, 601 (1984).
[14]H. Okamoto and T. B. Massalski, J. Phase Equilib. **4**, 190 (1983).
[15]S. A. Dayeh and S. T. Picraux, Nano Lett. **10**, 4032 (2010).
[16]Y. Wu, Y. Cui, L. Huynh, C. J. Barrelet, D. C. Bell, and C. M. Lieber, Nano Lett. **4**, 433 (2004).
[17]T. Hanrath and B. A. Korgel, Small **1**, 717 (2005).